Throughput Maximization for Multi-Hop Wireless Networks with Network-Wide Energy Constraint

Canming Jiang, Yi Shi, *Member, IEEE,* Y. Thomas Hou, *Senior Member, IEEE,*
Wenjing Lou, *Senior Member, IEEE,* and Hanif D. Sherali

***Abstract*—The cost of energy consumption is an important concern for network operators. In this paper, we study an energy-related problem that focuses on network-wide energy consumption. In the first part of this work, we study how to maximize throughput under a network-wide energy constraint. We formulate this problem as a mixed-integer nonlinear program (MINLP). This formulation differs from prior efforts as it considers a non-zero device power, which complicates the problem. We propose a novel piece-wise linear approximation to transform the nonlinear constraints into linear constraints. We prove that the solution developed under this approach is near-optimal with a guaranteed performance bound. In the second part, we generalize the problem in the first part via a multicriteria optimization framework, which simultaneously optimizes throughput and total network energy. We show how weakly Pareto-optimal solutions can characterize an optimal throughput-energy curve. We offer some interesting properties of the optimal throughput-energy curves, which are useful to both network operators and end-users. Our results fill in some important gaps in the current understanding on optimizing total network energy.**

***Index Terms*—Energy optimization, total network energy, network throughput, multicriteria optimization, multi-hop wireless networks.**

I. Introduction

ENERGY has been, and will remain, a fundamental concern for wireless networks. In this paper, we focus on total network energy (or network-wide energy), which is not a well studied area but is of critical importance to network operators. Specifically, we explore the following two problems: (i) How to maximize network throughput under a given total network energy constraint. The solution to this question will help network operators achieve the highest performance (throughput) under a given energy budget. (ii) How to simultaneously optimize both network throughput and network-wide energy consumption. This problem generalizes the first one and its solution allows us to understand the relationships and tradeoffs between network throughput and total network energy.

Manuscript received May 6, 2012; revised August 26 and December 20, 2012; accepted December 29, 2012. The associate editor coordinating the review of this paper and approving it for publication was C.-F. Chiasserini.

An abridged version of this paper [12] was presented at IEEE INFOCOM, Orlando, Florida, March 25–30, 2012.

C. Jiang, Y. Shi, and Y. T. Hou (corresponding author) are with the Bradley Department of Electrical and Computer Engineering, Virginia Tech, Blacksburg, VA 24061, USA (e-mail: {jcm, yshi, thou}@vt.edu).

W. Lou is with the Department of Computer Science, Virginia Tech, Falls Church, VA 22043, USA (e-mail: wjlou@vt.edu).

H. D. Sherali is with the Grado Department of Industrial and Systems Engineering, Virginia Tech, Blacksburg, VA 24061, USA (e-mail: hanifs@vt.edu).

Digital Object Identifier 10.1109/TWC.2013.013013.120636

We recognize that there is a wealth of literature on optimizing network throughput with energy constraints. A major thrust of these prior efforts was to develop various heuristic approaches for physical, link, and network layer operational schemes (see, e.g., [14], [21], [23]). This is in contrast to our work in this paper, which follows a formal optimization framework with the goal of offering a performance guarantee for the final solution.

Among related works that adopt formal optimization frameworks in studying network throughput maximization with energy consideration (see, e.g., [1], [9], [20]), we find that most of these works only consider per-link power constraints or per-node power constraints. Although such an approach is important to characterize local energy consumption, it cannot be easily extended to address problems for *network-wide* energy due to the complex inter-dependency among the layers.

Our work is complementary to a branch of previous work that addresses how to minimize network-wide energy consumption while satisfying some traffic demands (see, e.g., [15], [18]). These works are orthogonal to the problem that we study in the first part of this paper. In some sense, the problem studied in this paper is the dual to these existing works. However, a main departure from these works is our consideration of the device power, which introduces a new combinatorial aspect into the problem. As a result, our problem is much more difficult to solve, and hence a novel approximation approach that is asymptotically optimal is proposed in the paper. It will soon be clear that our mathematical formulation and proposed solution procedure differ from all seemingly similar prior efforts. Further, in the second part of this paper, we consider the joint optimization of throughput and network-wide energy based on *multicriteria optimization,* which is an area that is not well studied in network energy conservation contexts.

The main contributions of this paper are the following:

- First, we study how to maximize network throughput under a total network energy constraint. Our problem considers device power, which is relevant in practice. We show that this problem can be formulated as a mixed-integer nonlinear program (MINLP). To solve this problem efficiently, we exploit its mathematical structure and propose a novel piece-wise linear approximation that is asymptotically optimal. This approximation allows to transform the nonlinear constraints into linear constraints. We prove that the solution developed under this linear approximation is near-optimal in the sense that the performance gap between our solution and the optimal solution

(unknown) can be made arbitrary small as per required accuracy.

- Second, we generalize the problem in the first part by exploring the joint optimization of both network throughput and network energy consumption via a multicriteria optimization framework, i.e., by *maximizing* network throughput while *minimizing* network-wide energy consumption. The set of weakly Pareto-optimal points characterize an optimal throughput-energy curve. This curve shows how the maximum network throughput changes with the total network energy. We offer some interesting properties of this optimal throughput-energy curve, which are of importance to both network operators and end-users.
- Third, we conduct extensive numerical experiments to show the efficacy of our proposed approach and to validate our theoretical findings. We present numerical results for 50-node, 100-node, and 200-node networks. These results offer further insights in addition to validating our proposed solution procedure.

The remainder of this paper is organized as follows. In Section II, we describe our network model. In Section III, we study the problem of how to maximize network throughput under a given total network energy. In Section IV, we study how to optimize both network throughout and energy under a multicriteria framework. Section V presents numerical results, and Section VI concludes this paper.

II. Network Model

Consider a multi-hop wireless ad hoc network that is represented by a directed graph $\mathcal{G} = \{\mathcal{N}, \mathcal{L}\}$, where $\mathcal{N}$ and $\mathcal{L}$ are the sets of nodes and directional links, respectively. A link between two nodes exists if and only if the distance between the two is within a certain transmission range. If two nodes are not within one-hop of each other, then a node has to use multi-hops to relay messages. We assume orthogonal channels on all links (similar to that in [3], [13], [16]). This can be done by some interference avoidance mechanism (e.g., OFDMA). Note that orthogonal channels do not require as many channels as the number of active links in the network since one can reuse channels on links that are spatially far away from each other. This is called spatial reuse and is commonly used in wireless networks to improve channel efficiency. Note that designing a channel assignment algorithm to achieve orthogonality has been well studied in the literature and its discussion is beyond the scope of this paper.

We assume that there is a set $\mathcal{F}$ of active communication sessions in the network. Each session involves a single-source single-destination unicast flow. Denote $s(f)$ and $d(f)$ as the source and destination nodes of session $f \in \mathcal{F}$, respectively. To differentiate the importance of these user sessions, each session f is assigned a weight $w(f)$.[1] Let $r(f)$ be the data rate of session f. The network throughput U in this paper is represented by the sum of weighted session rates, which is given by $\sum_{f\in\mathcal{F}} w(f)\cdot r(f)$. Table I lists all the notation used in this paper.

[1]We assume that the weight of a flow is given *a priori* and is a constant. How to assign a weight to a flow is application-dependent (e.g., based on priority) and its discussion is beyond the scope of this paper.

TABLE I
Notation.

Symbol	Definition
B_l	Channel bandwidth on link l
c_l	Capacity of link l
d_l	Distance between link l's transmitting node and receiving node
$\mathcal{F}$	The set of user sessions in the network
$d(f)$	Destination node of session $f \in \mathcal{F}$
$\mathcal{L}$	The set of links in the network
$\mathcal{L}_i^{\mathrm{In}}$	The set of incoming links at node i
$\mathcal{L}_i^{\mathrm{Out}}$	The set of outgoing links at node i
h_l	Channel gain on link l
$\mathcal{N}$	The set of nodes in the network
p_l	Transmission power of link l
P_d	Device power consumption associated with an active link
P	$=\sum_{l\in\mathcal{L}}(p_l + y_l P_d)$, network-wide energy consumption rate
P_{net}	Network-wide energy budget
$r(f)$	Data rate of session $f \in \mathcal{F}$
$r_l(f)$	Data rate on link l that is attributed to session f
$s(f)$	Source node of session f
U	$=\sum_{f\in\mathcal{F}} w(f)r(f)$, the network throughput
$w(f)$	A weight assigned to session $f \in \mathcal{F}$
y_l	A binary variable indicating whether or not link l is active
η	Ambient Gaussian noise density

A. Energy Consumption and Power Control

When a wireless link is active for communication, its energy consumption includes transmission power at the transmitter (for data transmission over a distance), and device power at both the transmitter and the receiver (for encoding, modulation, decoding, demodulation, etc.) [5], [17]. Denote $p_l \geq 0$ as the transmission power at the transmitter for link l, which can be varied depending on transmission requirements. Let P_d be the constant device power when a link is active. Denote y_l as a binary variable indicating whether or not link l is active, i.e.,

$$y_l = \begin{cases} 1 & \text{if link } l \text{ is active;} \\ 0 & \text{otherwise.} \end{cases}$$

When a link is active, we utilize the power P_d; when a link is inactive, we do not. This behavior is readily modeled by multiplying P_d by y_l (the link activity indicator). Incorporating the transmission power p_l, the total power consumption rate of link l is therefore given by $p_l + y_l P_d$.

Assume that the maximum transmission power of a node is $P_{\max}$. Then, we have the following relationship between p_l and y_l:

$$p_l \leq y_l \cdot P_{\max} \quad (l \in \mathcal{L}) \,. \tag{1}$$

For all active links at a node, we have the following *node-level* transmission power constraint:

$$\sum_{l\in\mathcal{L}_i^{\mathrm{Out}}} p_l \leq P_{\max} \quad (i \in \mathcal{N}) \,, \tag{2}$$

where $\mathcal{L}_i^{\mathrm{Out}}$ is the set of potential outgoing links at node i.

Denote P as the total energy consumption rate on all active links in the network. Then, the network-wide energy consumption rate P can be written as $P = \sum_{l\in\mathcal{L}}(p_l + y_l P_d)$.

B. Routing and Link Capacity

To transport data from a source node to its destination node that is more than one-hop away, multi-hop relaying is necessary. Since single-path flow routing is overly restrictive and is likely suboptimal, we allow flow splitting so that data can be delivered along multi-path routes. We model multi-path flow routing as follows. Denote $r_l(f)$ as the amount of flow rate on link l that is attributed to session $f \in \mathcal{F}$. Denote $\mathcal{L}_i^{\rm In}$ as the set of potential incoming links at node i. If node i is the source node of session f, i.e., $i = s(f)$, then

$$\sum_{l \in \mathcal{L}_i^{\rm Out}} r_l(f) = r(f) \ . \tag{3}$$

If node i is an intermediate relay node of session f, i.e., $i \neq s(f)$ and $i \neq d(f)$, then

$$\sum_{l \in \mathcal{L}_i^{\rm Out}, l \neq (i,s(f))} r_l(f) = \sum_{m \in \mathcal{L}_i^{\rm In}, m \neq (d(f),i)} r_m(f) \ . \tag{4}$$

If node i is the destination node of session f, i.e., $i = d(f)$, then

$$\sum_{l \in \mathcal{L}_i^{\rm In}} r_l(f) = r(f) \ . \tag{5}$$

It can be easily verified that if (3) and (4) are satisfied, then (5) must be satisfied. As a result, it is sufficient to list only (3) and (4) in the formulation. It is worth pointing out that our multi-path routing model is a link-based model with variables $r_l(f)$ (the flow rate on link l that is attributed to session f) and $r(f)$ (the data rate of session f). The number of variables is polynomial of $O(|\mathcal{L}| \cdot |\mathcal{F}|)$, where $|\mathcal{L}|$ is the number of links in the network and $|\mathcal{F}|$ is the number of sessions in the network.

Under the above flow routing scheme, the aggregate flow rate on link l is $\sum_{f \in \mathcal{F}} r_l(f)$. Since the aggregate flow rate on any link cannot exceed the link's capacity, we have the following link capacity constraint:

$$\sum_{f \in \mathcal{F}} r_l(f) \leq c_l \quad (l \in \mathcal{L}) \ , \tag{6}$$

where c_l is the capacity of link l. Given that we are employing orthogonal channels among the links in the network, we have:

$$c_l = B_l \log_2(1 + \frac{p_l \cdot h_l}{\eta B_l}) \ , \tag{7}$$

where B_l is the bandwidth of link l under a given channel assignment, h_l is the channel gain between the transmitter and the receiver of link l, and η is the ambient Gaussian noise density. Combining (6) and (7), we have:

$$\sum_{f \in \mathcal{F}} r_l(f) \leq B_l \log_2(1 + \frac{p_l \cdot h_l}{\eta B_l}) \quad (l \in \mathcal{L}) \ . \tag{8}$$

Note that Constraint (8) couples the network flow variables (i.e., $r_l(f)$) and the physical layer power variable p_l over the links in the network.

III. Throughput Maximization under a Total Network Energy Constraint

In this section, we study how to maximize network throughput under a given network-wide energy budget. This problem is motivated by the scenario where we have a strict total energy consumption limit in the network. For example, in a wireless mesh network, we may impose a total energy consumption constraint due to a given operating budget on energy, since the operational cost is directly proportional to energy consumption. The question that we pose is: Given the network-wide energy operating budget $P_{\rm net}$, i.e.,

$$P = \sum_{l \in \mathcal{L}} (p_l + y_l P_d) \leq P_{\rm net}, \tag{9}$$

how can we adjust the power on each link and perform multi-path routing for each session so as to maximize the network throughput?

Mathematically, this problem can be formulated as follows:

$$\begin{aligned} \textbf{OPT:} \quad \max \quad & U = \sum_{f \in \mathcal{F}} w(f) r(f) \\ \text{s.t.} \quad & \text{Link power constraint: } (1) \\ & \text{Node power constraint: } (2) \\ & \text{Flow balance: } (3), (4) \\ & \text{Link flow constraint: } (8) \\ & \text{Total network energy constraint: } (9) \\ & \text{Variables } y_l \in \{0,1\}, p_l, r_l(f), r(f) \geq 0 \\ & \qquad\qquad (l \in \mathcal{L}, f \in \mathcal{F}) \ , \end{aligned}$$

where y_l is a binary variable; p_l, $r(f)$, and $r_l(f)$ are continuous variables, and all the other parameters are constants. OPT is a mixed-integer nonlinear program (MINLP), which in general is NP-hard [10].

Note that the network-wide energy constraint complicates the overall problem by requiring binary variables. These binary variables are necessary due to our consideration of the device power P_d. If such a device power is neglected, then the binary variables can be removed, and the problem becomes a convex problem, which can be readily solved. But in practice, such a device power should be considered. Mathematically, this consideration differentiates this paper from previous works in this area.

MINLP problems are known to be difficult due to the combinatorial nature of mixed-integer programs and the difficulty in solving nonlinear programs. Note that there exist some techniques to address *general* MINLP problems (e.g., outer-approximation methods [7], branch-and-bound [8], extended cutting plane methods [22], and generalized Benders' decomposition [11]). But these techniques do not exploit our problem-specific structures and properties, and hence can only handle small-sized problems.

In this paper, we exploit the unique mathematical structure of our MINLP problem and develop a novel near-optimal solution procedure with a performance guarantee. Note that in Problem OPT, the only nonlinear constraints are the link capacity constraints (8), which involve the $\log$ function. To address this problem, we propose a piece-wise linear approximation technique to transform the nonlinear constraints to

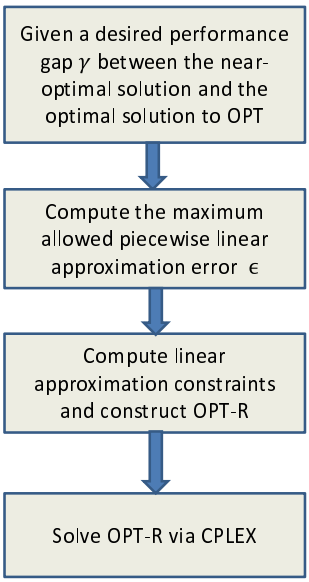

Fig. 1. A flow-chart for obtaining a near-optimal solution to OPT.

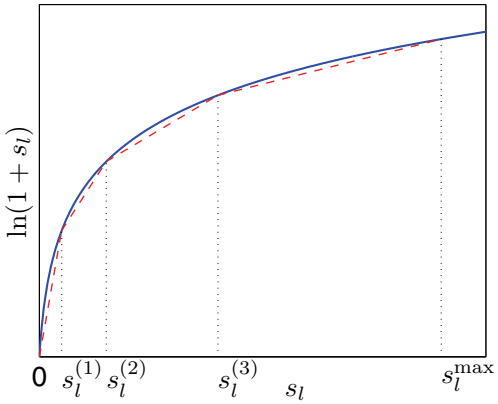

Fig. 2. An illustration of piece-wise linear approximation with four linear segments.

linear constraints. Our main idea is as follows. We first use a set of linear segments to approximate the log term in (8) while ensuring that the linear approximation error does not exceed a specific threshold ϵ. Subsequently, the nonlinear constraints in OPT are replaced by a set of linear constraints. Denote the linearized optimization problem as OPT-R, which is a mixed-integer linear problem (MILP). Since MILP problems are relatively easier to solve than MINLP problems, we can efficeintly apply a solver such as CPLEX [4] to obtain a solution efficiently.

We will show that solving OPT-R gives us a near-optimal solution to the original problem OPT. Denote γ as the desired performance gap for the near-optimal solution, i.e., the difference in the objective values between the optimal solution and the near-optimal solution to OPT. We analyze the relationship between the performance gap γ and the linear approximation error ϵ (see details in Section III-B). Specifically, for a desired performance gap γ, we compute the maximum allowed linear approximation error ϵ, and accordingly, we derive the linear approximation constraints and construct OPT-R (see details in Section III-A). The solution to OPT-R then provides a near-optimal solution with the performance guarantee γ. We summarize the above steps in Fig. 1, and we provide details for the steps in the remainder of this section.

A. Piece-wise Linear Approximation

We can rewrite the nonlinear constraint in (8) as follows:

$$\sum_{f\in\mathcal{F}} r_l(f) \le \frac{B_l}{\ln 2}\ln(1+\frac{p_l\cdot h_l}{\eta B_l}). \tag{10}$$

To simplify notation, we denote

$$s_l \equiv \frac{p_l h_l}{\eta B_l}\ . \tag{11}$$

Then, the nonlinear term in (10) can be written as $\ln(1+s_l)$. The range of s_l is $[0, s_l^{\max}]$, with $s_l^{\max} = (P_{\max}h_l)/(\eta B_l)$.

The essence of our proposed piece-wise linear approximation is to use a set of consecutive linear segments to approximate $\ln(1+s_l)$ for $s_l \in [0, s_l^{\max}]$ (see Fig. 2). Denote ϵ as the maximum allowed error for this linear approximation and let K_l be the number of linear segments needed to meet this error requirement (K_l will be determined later). Denote $s_l^{(k)}, k = 0, 1, \ldots, K_l$ as the s_l-axis values of the endpoints for these K segments, with $s_l^{(0)} \equiv 0$ and $s_l^{(K_l)} \equiv s_l^{\max}$.

A naive approach to generate a linear approximation is to have $s_l^{(k)}, k = 0, \ldots, K_l$, evenly distributed between $[0, s_l^{\max}]$. When setting K_l sufficiently large, the linear approximation error requirement will be satisfied. Although this approach is straightforward and easy to implement, it will generate too many linear segments to approximate $\ln(1+s_l)$. Note that the derivative of $\ln(1+s_l)$ decreases as s_l increases. This motivates us to enlarge the size of an interval as s_l increases. Thus, we want to pursue an algorithm that optimally divides the K_l intervals within $[0, s_l^{\max}]$. By "optimally", we refer to finding the *minimum* K_l such that the maximum approximation error of each line segment is no more than ϵ.

Denote $m_l^{(k)}$ as the slope of the k-th linear segment, i.e.,

$$m_l^{(k)} = \frac{\ln(1+s_l^{(k)}) - \ln(1+s_l^{(k-1)})}{s_l^{(k)} - s_l^{(k-1)}}. \tag{12}$$

Denote $g_l^{(k)}(s_l)$ as the k-th linear approximation segment (see Fig. 3), which can be represented as follows:

$$g_l^{(k)}(s_l) = m_l^{(k)}\cdot\left(s_l - s_l^{(k-1)}\right) + \ln\left(1+s_l^{(k-1)}\right), \quad \text{for } s_l^{(k-1)} \le s_l \le s_l^{(k)}. \tag{13}$$

Our algorithm computes the values of $s_l^{(0)}, \ldots, s_l^{(K_l)}$ sequentially (for a given ϵ) based on Algorithm 1 as follows:

Algorithm 1: Initialization: $k := 0$ and $s_l^{(0)} := 0$.

1) $k := k + 1$.
2) Compute $m_l^{(k)}$ that satisfies
$$-\ln(m_l^{(k)}) + m_l^{(k)}(1+s_l^{(k-1)}) - 1 - \ln(1+s_l^{(k-1)}) = \epsilon. \tag{14}$$
3) With $m_l^{(k)}$, compute $s_l^{(k)}$ that satisfies (12).

4) If $s_l^{(k)} < s_l^{\max}$, go to Step 1.
5) $K_l := k$; $s_l^{(K_l)} := s_l^{\max}$.
6) Update $m_l^{(K_l)}$ using (12).

The values of $m_l^{(k)}$ in (14) and $s_l^{(k)}$ in (12) can be solved by numerical methods such as the bisection method or Newton's method [19, Chapter 2].

Our linear approximation method (Algorithm 1) satisfies the linear approximation error requirement with the minimum number of linear segments to approximate $\ln(1+s_l)$ for $s_l \in [0, s_l^{\max}]$. We formally state these claims in the following two lemmas.

Lemma 1: For the piece-wise linear approximation generated by Algorithm 1, the maximum approximation error of each linear segment is at most ϵ.

Proof Denote $\epsilon_l^{(k)}$ as the maximum linear approximation error for the k-th linear segment, i.e.,

$$\begin{aligned}\epsilon_l^{(k)} &= \max_{s_l^{(k-1)} \le s_l \le s_l^{(k)}} \left| \ln(1+s_l) - g_l^{(k)}(s_l) \right| \\ &= \max_{s_l^{(k-1)} \le s_l \le s_l^{(k)}} \left\{ \ln(1+s_l) - g_l^{(k)}(s_l) \right\},\end{aligned}$$

where the equality holds since $\ln(1+s_l)$ is a concave function of s_l and all linear segments lie beneath the $\ln(1+s_l)$ curve.

Consider the k-th linear segment. Referring to Fig. 3, we can move $g_l^{(k)}(s_l)$ upward until it is tangential to the $\ln(1+s_l)$ curve. It is easy to see (by differentiating the above concave function and setting to zero) that the tangential point achieves the maximum approximation error $\epsilon_l^{(k)}$. Denote $\hat{s}_l^{(k)}$ as the s_l-axis value of that tangential point. Since the derivative of $\ln(1+s_l)$ is $\frac{1}{1+s_l}$, we have $\frac{1}{1+\hat{s}_l^{(k)}} = m_l^{(k)}$, i.e,

$$\hat{s}_l^{(k)} = \frac{1}{m_l^{(k)}} - 1, \tag{15}$$

where $m_l^{(k)}$ is the slope of the linear segment $g_l^{(k)}(s_l)$. Therefore, the maximum approximation error $\epsilon_l^{(k)}$ can be written as:

$$\begin{aligned}\epsilon_l^{(k)} &= \ln(1+\hat{s}_l^{(k)}) - g_l^{(k)}(\hat{s}_l^{(k)}) \\ &= \ln(1+\hat{s}_l^{(k)}) - [m_l^{(k)} \cdot (\hat{s}_l^{(k)} - s_l^{(k-1)}) + \ln(1+s_l^{(k-1)})] \\ &= \ln\left(1 + \frac{1}{m_l^{(k)}} - 1\right) \\ &\quad - \left\{ m_l^{(k)} \cdot \left[\frac{1}{m_l^{(k)}} - 1 - s_l^{(k-1)} \right] + \ln(1+s_l^{(k-1)}) \right\} \\ &= -\ln(m_l^{(k)}) + m_l^{(k)}(1+s_l^{(k-1)}) - 1 - \ln(1+s_l^{(k-1)}),\end{aligned}$$

where the second equality holds due to (13) and the third equality holds due to (15).

In Algorithm 1, we set $-\ln(m_l^{(k)}) + m_l^{(k)}(1+s_l^{(k-1)}) - 1 - \ln(1+s_l^{(k-1)}) = \epsilon$. Thus, the maximum linear approximation error for the k-th linear segment is ϵ. This result holds for all $k = 1, \cdots, K_l$. This completes the proof. □

Lemma 2: For a given approximation error bound ϵ for each linear segment, Algorithm 1 minimizes the number of linear segments to approximate $\ln(1+s_l)$ for $s_l \in [0, s_l^{\max}]$.

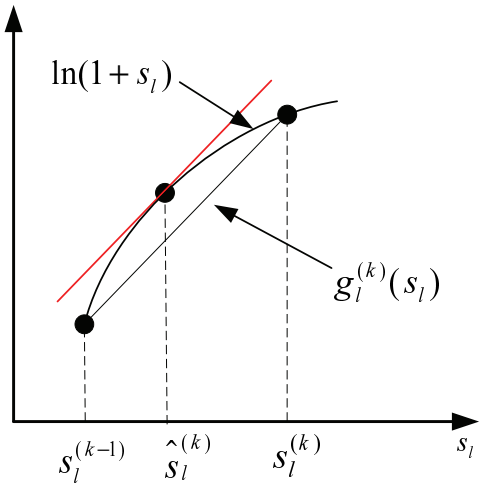

Fig. 3. An illustration of the maximum approximation error for the k-th linear segment.

The proof of Lemma 2 is given in the appendix.

With the proposed piece-wise linear approximation of $\ln(1+s_l)$, Constraint (8) can be replaced by the following set of constraints:

$$\sum_{f \in \mathcal{F}} r_l(f) \le \frac{B_l}{\ln 2} g_l^{(k)}(s_l) \qquad (k = 1, \ldots, K_l, l \in \mathcal{L}),$$

where s_l and $g_l^{(k)}(s_l)$ are given by (11) and (13), respectively. Substituting (11) and (13) into the above equation, we have

$$\sum_{f \in \mathcal{F}} r_l(f) \le \frac{B_l}{\ln 2} \left\{ m_l^{(k)} \left[\frac{p_l h_l}{\eta B_l} - s_l^{(k-1)} \right] + \ln\left[1 + s_l^{(k-1)}\right] \right\} \qquad (k = 1, \ldots, K_l, l \in \mathcal{L}). \tag{16}$$

By replacing the nonlinear constraints in (8) with the set of linear constraints in (16), we obtain the following revised formulation for OPT, which we denote as OPT-R:

OPT-R: max $\sum_{f \in \mathcal{F}} w(f) r(f)$

s.t. Link power constraint: (1)
Node power constraint: (2)
Flow balance: (3), (4)
Linearized link flow constraint: (16)
Total network energy constraint: (9)
Variables $y_l \in \{0,1\}, p_l, r_l(f), r(f) \ge 0$ $(l \in \mathcal{L}, f \in \mathcal{F})$.

We have the following lemma on the relationship between OPT-R and OPT.

Lemma 3: A feasible solution to OPT-R is a feasible solution to OPT.

The proof of Lemma 3 is given in the appendix.

B. A Near-Optimal Solution

OPT-R is a mixed-integer linear program (MILP) and can be solved effectively by a commercial solver such as CPLEX [4]. We now provide a bound for the gap between the optimal

objective values of OPT and OPT-R, despite that the optimal objective value of OPT is not available.

To proceed, we need the following notation. For a given power assignment (y_l, p_l) to OPT (i.e., satisfying Constraints (1), (2), (9)), define $\bar{\mathbf{x}} = (\bar{r}(f), \bar{r}_l(f), y_l, p_l)$ as a feasible solution to OPT, where $(\bar{r}(f), \bar{r}_l(f))$ is the optimal solution to the following linear program (LP).

$$\begin{aligned}
&\mathbf{OPT}(y_l, p_l):\\
&\max \sum_{f\in\mathcal{F}} w(f)r(f)\\
&\text{s.t.} \sum_{l\in\mathcal{L}_i^{\text{Out}}} r_l(f) = r(f) \;\; (f\in\mathcal{F}, i\in\mathcal{N}, i = s(f))\\
&\qquad \sum_{l\in\mathcal{L}_i^{\text{Out}}, l\neq(i,s(f))} r_l(f) = \sum_{l\in\mathcal{L}_i^{\text{In}}, l\neq(d(f),i)} r_l(f)\\
&\qquad\qquad (f\in\mathcal{F}, i\in\mathcal{N}, i\neq s(f), d(f))\\
&\qquad \sum_{f\in\mathcal{F}} r_l(f) \le \bar{c}_l \;\; (l\in\mathcal{L})\\
&\qquad r_l(f), r(f) \ge 0 \;\; (l\in\mathcal{N}, f\in\mathcal{F}),
\end{aligned}$$

where $\bar{c}_l = B_l \log_2(1 + \frac{p_l \cdot h_l}{\eta B_l})$. Note that OPT$(y_l, p_l)$ is an LP once we fix the power variables in OPT to the values (y_l, p_l).

For a feasible solution $\bar{\mathbf{x}} = (\bar{r}(f), \bar{r}_l(f), y_l, p_l)$ to OPT, we define a feasible solution $\mathbf{x}^\dagger = (r^\dagger(f), r_l^\dagger(f), y_l, p_l)$ to OPT-R as follows. In $\mathbf{x}^\dagger \equiv (r^\dagger(f), r_l^\dagger(f), y_l, p_l)$, we let $(r^\dagger(f), r_l^\dagger(f))$ be the optimal flow routing solution to OPT-R for the given (y_l, p_l). That is, $(r^\dagger(f), r_l^\dagger(f))$ is the optimal solution to the following LP in which the power variables in OPT-R are fixed at the given values (y_l, p_l).

$$\begin{aligned}
&\mathbf{OPT\text{-}R}(y_l, p_l):\\
&\max \sum_{f\in\mathcal{F}} w(f)r(f)\\
&\text{s.t.} \sum_{l\in\mathcal{L}_i^{\text{Out}}} r_l(f) = r(f) \;\; (f\in\mathcal{F}, i\in\mathcal{N}, i = s(f))\\
&\qquad \sum_{l\in\mathcal{L}_i^{\text{Out}}, l\neq(i,s(f))} r_l(f) = \sum_{l\in\mathcal{L}_i^{\text{In}}, l\neq(d(f),i)} r_l(f)\\
&\qquad\qquad (f\in\mathcal{F}, i\in\mathcal{N}, i\neq s(f), d(f))\\
&\qquad \sum_{f\in\mathcal{F}} r_l(f) \le c_l^\dagger \;\; (l\in\mathcal{L}),
\end{aligned}$$

where $c_l^\dagger$ is a linear approximation of link l's capacity given the transmission power p_l.

Remark 1: Recall that we use Constraint (16) to replace Constraint (8) in OPT-R. When link l's power is fixed at p_l, we can determine which line segment is involved in the linear approximation of $\ln(1+s_l)$. Suppose that the k-th linear segment is used, i.e., $s_l^{(k-1)} \le \frac{p_l \cdot h_l}{\eta B_l} \le s_l^{(k)}$. Then, link l's approximated capacity can be written as $c_l^\dagger = \frac{B_l}{\ln 2} \cdot g_l^{(k)}(\frac{p_l \cdot h_l}{\eta B_l})$. □

To quantify the performance gap between our solution to OPT-R and the optimal solution to OPT, we will first show that for any feasible power assignment (p_l, y_l), the gap between the objective values corresponding to $\bar{\mathbf{x}}$ and $\mathbf{x}^\dagger$ is at most $\frac{\epsilon}{\ln 2} \max_{f\in\mathcal{F}}\{w(f)\} \sum_{l\in\mathcal{L}} B_l$. Then, we will show that the gap between the optimal objective values of OPT and OPT-R is also bounded by $\frac{\epsilon}{\ln 2} \max_{f\in\mathcal{F}}\{w(f)\} \sum_{l\in\mathcal{L}} B_l$.

We find that this gap can be characterized in the dual domain to Problems OPT(y_l, p_l) and OPT-R(y_l, p_l).

Lemma 4: For given (y_l, p_l), denote $\bar{z}$ and $z^\dagger$ as the objective values of the solutions $\bar{\mathbf{x}}$ (to OPT) and $\mathbf{x}^\dagger$ (to OPT-R), respectively. Then we have $\bar{z} - z^\dagger \le \frac{\epsilon}{\ln 2} \max_{f\in\mathcal{F}}\{w(f)\} \sum_{l\in\mathcal{L}} B_l$.

Proof Note that $\bar{z}$ is the optimal objective value of OPT(y_l, p_l) and $z^\dagger$ is the optimal objective value of OPT-R(y_l, p_l). Consider the dual problems of OPT(y_l, p_l) and OPT-R(y_l, p_l), denoted by D(y_l, p_l) and D-R(y_l, p_l), respectively. Note that D(y_l, p_l) and D-R(y_l, p_l) have the same constraints, but different objective functions.

Denote the dual variables corresponding to the first group of constraints in OPT(y_l, p_l) and OPT-R(y_l, p_l) as $u(f), f \in \mathcal{F}$. Denote the dual variables corresponding to the second group of constraints in OPT(y_l, p_l) and OPT-R(y_l, p_l) as $v_i(f), f \in \mathcal{F}, i \in \mathcal{N}, i \neq s(f), d(f)$. Denote the dual variables corresponding to the third group of constraints in OPT(y_l, p_l) and OPT-R(y_l, p_l) as $q_l, l \in \mathcal{L}$. Then, D(y_l, p_l) can be written as follows:

$$\begin{aligned}
&\min \sum_{l\in\mathcal{L}} \bar{c}_l q_l\\
&\text{s.t.} -u(f) \ge w(f) \;\; (f\in\mathcal{F})\\
&\quad u(f) - v_j(f) + q_l \ge 0\\
&\qquad (l \equiv (s(f), j) \in \mathcal{L}, j \neq d(f), f\in\mathcal{F})\\
&\quad v_i(f) - v_j(f) + q_l \ge 0\\
&\qquad (l \equiv (i, j) \in \mathcal{L}, i \neq s(f), i \neq d(f), j \neq d(f), f\in\mathcal{F})\\
&\quad v_i(f) + q_l \ge 0 \; (l \equiv (i, d(f)) \in \mathcal{L}, f\in\mathcal{F})\\
&\quad u(f), v_i(f) \text{ unrestricted}, q_l \ge 0\\
&\qquad\qquad (f\in\mathcal{F}, i\in\mathcal{N}\backslash\{s(f), d(f)\}, l\in\mathcal{L}),
\end{aligned}$$

where $v_i(f) \equiv u(f)$ if $i \equiv s(f)$ in the last dual inequality constraint. The dual problem D-R(y_l, p_l) can be written as

$$\begin{aligned}
\text{D-R}(y_l, p_l): \quad &\min \sum_{l\in\mathcal{L}} c_l^\dagger q_l\\
&\text{s.t. Same constraints as D}(y_l, p_l).
\end{aligned}$$

If $(q_l^*, l\in\mathcal{L})$ is (part of) an optimal solution to D-R(y_l, p_l), then since both D(y_l, p_l) and D-R(y_l, p_l) have the same feasible region, we have

$$\bar{z} - z^\dagger \le \sum_{l\in\mathcal{L}} \bar{c}_l q_l^* - \sum_{l\in\mathcal{L}} c_l^\dagger q_l^* = \sum_{l\in\mathcal{L}} (\bar{c}_l - c_l^\dagger) q_l^* .$$

Note that the gap between $\bar{c}_l$ and $c_l^\dagger$ is

$$\bar{c}_l - c_l^\dagger \le \frac{B_l}{\ln 2}\epsilon,$$

since the maximum error of our linear approximation is ϵ. Thus, we have

$$\bar{z} - z^\dagger \le \frac{\epsilon}{\ln 2} \sum_{l\in\mathcal{L}} B_l q_l^* . \tag{17}$$

By the marginal rate of change interpretation of dual variables [2], q_l^* is bounded above by the largest possible change

in the optimal objective value of Problem OPT-R(y_l, p_l) with respect to the right-hand side c_l^+. But since a small marginal Δ-change (say, increase) in the capacity of any link can at most push an extra Δ units of flows between sources and destinations, and thus increase the objective value by at most $\max_{f\in\mathcal{F}}\{w(f)\}$, we have that

$$q_l^* \le \max_{f\in\mathcal{F}}\{w(f)\}\ . \tag{18}$$

Combining (17) and (18) gives us

$$\bar{z} - z^\dagger \le \frac{\epsilon}{\ln 2}\sum_{l\in\mathcal{L}} B_l \max_{f\in\mathcal{F}}\{w(f)\} = \frac{\epsilon}{\ln 2}\max_{f\in\mathcal{F}}\{w(f)\}\sum_{l\in\mathcal{L}} B_l\ .$$

This completes the proof. □

We are now ready to characterize the performance gap between the optimal objective values of OPT-R and OPT.

Theorem 1: The gap between the optimal objective values of OPT and OPT-R is no more than $\frac{\epsilon}{\ln 2}\max_{f\in\mathcal{F}}\{w(f)\}\sum_{l\in\mathcal{L}} B_l$.

Proof Denote $\mathbf{x}^*$ and z^* as the optimal solution and the optimal objective value of OPT, respectively. From Lemma 4, since $\mathbf{x}^*$ is a particular case of $\bar{\mathbf{x}}$, we know that there exists a feasible solution $\mathbf{x}_R$ to OPT-R corresponding to $\mathbf{x}^*$ such that the performance gap between $\mathbf{x}^*$ and $\mathbf{x}_R$ is at most $\frac{\epsilon}{\ln 2}\max_{f\in\mathcal{F}}\{w(f)\}\sum_{l\in\mathcal{L}} B_l$. Denote z_R as the objective value of the solution $\mathbf{x}_R$ to OPT-R. Then, we have

$$z^* - z_R \le \frac{\epsilon}{\ln 2}\max_{f\in\mathcal{F}}\{w(f)\}\sum_{l\in\mathcal{L}} B_l. \tag{19}$$

Denote z_R^* as the optimal objective value of OPT-R. Since z_R is the objective value of a feasible solution to OPT-R while z_R^* is the optimal objective value of OPT-R, we have

$$z_R^* \ge z_R. \tag{20}$$

Combining (19) and (20), we have $z^* - z_R^* \le \frac{\epsilon}{\ln 2}\max_{f\in\mathcal{F}}\{w(f)\}\sum_{l\in\mathcal{L}} B_l$. □

Based on Theorem 1, the following algorithm prescribes a near-optimal solution to OPT with a performance guarantee.

Algorithm 2: Input: Given a desired performance gap γ for the solution to OPT.

1) Compute ϵ based on
$$\frac{\epsilon}{\ln 2}\max_{f\in\mathcal{F}}\{w(f)\}\sum_{l\in\mathcal{L}} B_l = \gamma. \tag{21}$$
2) Compute $m_l^{(k)}$ and $s_l^{(k)}$ by Algorithm 1.
3) Construct OPT-R based on $m_l^{(k)}$ and $s_l^{(k)}$.
4) Solve OPT-R optimally using an MILP package (e.g., CPLEX).

Upon the completion of Algorithm 2, we have a near-optimal solution to OPT with a guaranteed performance bound (no more than γ from the optimal objective value).

IV. Maximizing Throughput and Minimizing Network-wide Energy

In the previous section, we have shown how to maximize network throughput while satisfying a given total network energy budget. The problem was formulated as a *single objective* optimization problem OPT. In this section, we go one step further. We are interested in maximizing network throughput while minimizing energy consumption. We cast this problem as a *multicriteria* optimization problem with two objectives. Mathematically, this problem can be written as follows:

$$\begin{aligned}
\textbf{MP:}\quad & \max \quad \sum_{f\in\mathcal{F}} w(f)r(f)\\
& \min \quad \sum_{l\in\mathcal{L}}(p_l + y_l P_d)\\
& \text{s.t.} \quad \text{Link power constraint: } (1)\\
& \qquad\quad \text{Node power constraint: } (2)\\
& \qquad\quad \text{Flow balance: } (3),(4)\\
& \qquad\quad \text{Link flow constraint: } (8)\\
& \qquad\quad \text{Variables } y_l \in \{0,1\}, p_l, r_l(f), r(f) \ge 0\\
& \qquad\qquad\qquad (l\in\mathcal{L}, f\in\mathcal{F}).
\end{aligned}$$

As we can see, minimizing the network-wide energy consumption and maximizing the network throughput (U) are two conflicting objectives. For such a problem, it is in general not possible to find a single feasible solution that is optimal for both objectives at the same time. For example, when P is minimized (i.e., equals 0), U is also 0 but is not maximized. Therefore, it is important to clarify what we mean by optimal solutions.

In this paper, we are interested in finding so-called weakly Pareto-optimal solutions [6]. Such solutions are desirable in the sense that it is impossible to improve the performance of both objectives simultaneously. Specifically, we say that (P^*, U^*) is a weakly Pareto-optimal solution to Problem MP if there does not exist another solution to Problem MP with (P, U) such that $P < P^*$ and $U > U^*$.

To find weakly Pareto-optimal solutions, we transform the multicriteria optimization problem into a single objective optimization problem. This can be done by moving the second objective (i.e., $\sum_{l\in\mathcal{L}}(p_l + y_l P_d)$) into the constraints as follows:

$$\begin{aligned}
\textbf{SP}(P_{\text{net}})\textbf{:}\quad & \max \quad \sum_{f\in\mathcal{F}} w(f)r(f)\\
& \text{s.t.} \quad \sum_{l\in\mathcal{L}}(p_l + y_l P_d) \le P_{\text{net}}\\
& \qquad\quad \text{Link power constraint: } (1)\\
& \qquad\quad \text{Node power constraint: } (2)\\
& \qquad\quad \text{Flow balance: } (3),(4)\\
& \qquad\quad \text{Link flow constraint: } (8)\\
& \qquad\quad \text{Variables } y_l \in \{0,1\}, p_l, r_l(f), r(f) \ge 0\\
& \qquad\qquad\qquad (l\in\mathcal{L}, f\in\mathcal{F}).
\end{aligned}$$

We see that this single objective optimization problem is precisely the same as OPT that we studied earlier. For a fixed value of P_{net}, solving SP(P_{net}) will give us *one* weakly Pareto-optimal point for Problem MP [6]. By varying P_{net} from 0 to $P_{\text{net}}^{\max} = |\mathcal{L}|\cdot(P_{\max} + P_d)$, we can obtain all weakly Pareto-optimal points. These points provide a mapping from the network-wide energy budget P_{net} to the maximum

network throughput U, which we denote as $\pi : P_{\rm net} \to U$. This mapping $U = \pi(P_{\rm net})$ provides an optimal throughput-energy curve, which characterizes how the maximum network throughput changes as the total network-wide energy consumption rate varies. This curve is useful for network operators to glean a holistic view of the entire optimal trade-off curve and decide which point to choose so as to meet their specific needs.

There are several interesting properties about this optimal throughput-energy curve $U = \pi(P_{\rm net})$, as given in Property 1 below.

Property 1: The optimal throughput-energy curve $U = \pi(P_{\rm net})$ has the following properties:

1) $\pi(P_{\rm net})$ is a nondecreasing function of $P_{\rm net}$.
2) $\pi(P_{\rm net})$ has a starting point $(P_{\rm start}, 0)$, i.e., $\pi(P_{\rm net}) = 0$ for $P_{\rm net} \le P_{\rm start}$ and $\pi(P_{\rm net}) > 0$ for $P_{\rm net} > P_{\rm start}$.
3) There is a saturation point $(P_{\rm sat}, U_{\rm sat})$ for $\pi(P_{\rm net})$, i.e., $\pi(P_{\rm net}) = U_{\rm sat}$ for $P_{\rm net} \ge P_{\rm sat}$.

Proof We prove each of these properties as follows.

1) Assume $P_{\rm net}^{(1)} < P_{\rm net}^{(2)}$. We need to show that $U(P_{\rm net}^{(1)}) \le U(P_{\rm net}^{(2)})$. Note that $U(P_{\rm net}^{(1)})$ and $U(P_{\rm net}^{(2)})$ are the optimal objectives of SP($P_{\rm net}^{(1)}$) and SP($P_{\rm net}^{(2)}$), respectively. Since $P_{\rm net}^{(1)} < P_{\rm net}^{(2)}$, the feasible region of SP($P_{\rm net}^{(1)}$) is contained within the feasible region of SP($P_{\rm net}^{(2)}$). Thus, we have $U(P_{\rm net}^{(1)}) \le U(P_{\rm net}^{(2)})$.
2) Such a starting point exists because when a link is active, it must consume a constant power P_d. For a session to have positive throughput, it must activate all the links along the path that are used by this session for transporting data. Thus, $P_{\rm start}$ can be determined by the session that uses the minimum number of hops from its source to its destination. Denote by m_f the minimum possible hops for session f. Then, $P_{\rm start}$ can be written as $P_{\rm start} = P_d \cdot \min\{m_f : f \in \mathcal{F}\}$.
3) We prove this property by construction. We first compute the saturation point $(P_{\rm sat}, U_{\rm sat})$ without the network-wide energy constraint. That is, we solve the following optimization problem:

$$\begin{aligned} \max \quad & \sum_{f\in\mathcal{F}} w(f)r(f) \\ \text{s.t.} \quad & \text{Constraints } (1),(2),(3),(4),(8). \\ & y_l \in \{0,1\}, p_l, r_l(f), r(f) \ge 0 \ \ (l \in \mathcal{L}, f \in \mathcal{F}) \ . \end{aligned}$$

The optimal objective value of the above problem is $U_{\rm sat}$. $U_{\rm sat}$ cannot be infinite, since the transmission power at a node has a threshold $P_{\max}$, which guarantees that the link capacity is finite, and hence the throughput is finite. Once we obtain $U_{\rm sat}$, we can determine the minimum energy $P_{\rm sat}$ that achieves $U_{\rm sat}$ by solving the following optimization problem:

$$\begin{aligned} \min \quad & \sum_{l\in\mathcal{L}} (p_l + y_l P_d) \\ \text{s.t.} \quad & \sum_{f\in\mathcal{F}} w(f)r(f) = U_{\rm sat} \\ & \text{Constraints } (1),(2),(3),(4),(8). \\ & y_l \in \{0,1\}, p_l, r_l(f), r(f) \ge 0 \ \ (l \in \mathcal{L}, f \in \mathcal{F}) \ . \end{aligned}$$

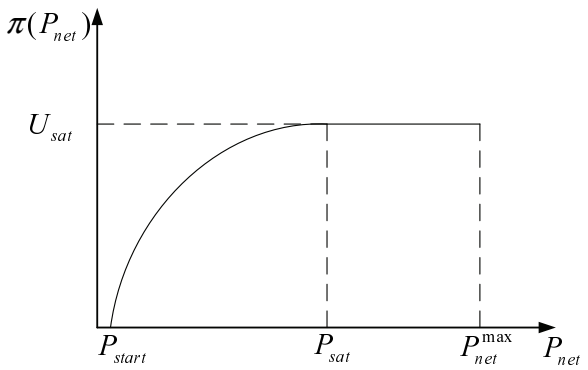

Fig. 4. An illustration of optimal throughput-energy curve.

Note that $P_{\rm sat}$ is the minimum energy consumption level that achieves $U_{\rm sat}$. When $P_{\rm net}$ is greater than this value, the maximum network throughput remains as $U_{\rm sat}$, i.e., $U = \pi(P_{\rm net})$ becomes flat for $P_{\rm net} \ge P_{\rm sat}$. □

Based on Property 1, Fig. 4 illustrates a typical optimal throughput-energy curve for a multi-hop wireless network.

V. Numerical Results

In this section, we present some numerical results to illustrate our approach in Sections III and IV.

A. Simulation Settings

We consider the following network topologies:

- a 50-node network deployed in a 1000 × 1000 square area;
- a 100-node network deployed in a 1500 × 1500 square area;
- a 200-node network deployed in a 2000 × 2000 square area.

The topologies of the 50-node, 100-node, and 200-node networks are shown in Figures 5, 6, and 7, respectively. We assume that all units are normalized with appropriate dimensions. We assume that the maximum transmission range is 200 and that the maximum transmission power is $P_{\max}$ = 2. We assume a node device power consumption of P_d = 0.2, unless specified otherwise.[2] The channel bandwidth is $B_l = 1$ for all links and the channel gain is $h_l = d_l^{-4}$, where d_l is the distance between link l's transmitting node and receiving node.

B. Results for the 50-node Network

Within this network, we assume that there are $|\mathcal{F}| = 5$ user sessions, with the source and destination nodes for each session chosen randomly. Table II lists the source node, destination node, and weight for each session in the network.

[2]In wireless mesh networks, the peak transmission power $P_{\max}$ is usually several Watts (2-3W), i.e., transmission power is between 0 and this $P_{\max}$ value, and the constant device power P_d is usually several hundreds mWatts (100-300 mW).

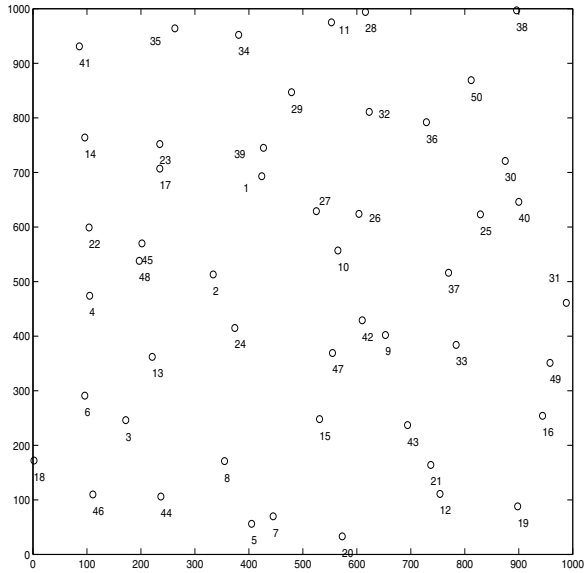

Fig. 5. The topology for a 50-node network.

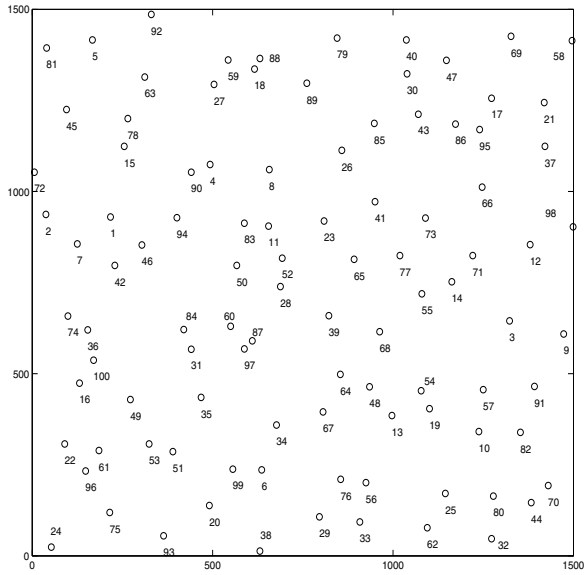

Fig. 6. The topology for a 100-node network.

1) Near-Optimal Solution for OPT: In this case study, we assume that the maximum network-wide energy consumption rate is given by $P_{\text{net}} = 40$. We set the maximum acceptable performance gap between the optimal objective values of OPT and the linear approximation OPT-R as $\gamma = 0.1$, and apply Algorithm 2. Based on (21), we compute $\epsilon = \frac{\gamma \ln 2}{\max_{f \in \mathcal{F}}\{w(f)\} \sum_{l \in \mathcal{L}} B_l} = 0.000393$, and thus compute the piece-wise linear approximation according to Algorithm 1. We then use CPLEX to solve OPT-R. The resulting maximum network throughput is $U = 22.32$. The achieved session data rates are $r_1 = 4.53$, $r_2 = 6.45$, $r_3 = 9.06$, $r_4 = 4.13$, and $r_5 = 6.79$. Our algorithm gives power control and flow routing solutions for the network. We list the power assignment for each active link in Table III, and the flow routing results in Table IV.

The above numerical results were obtained when $P_d = 0.2$.

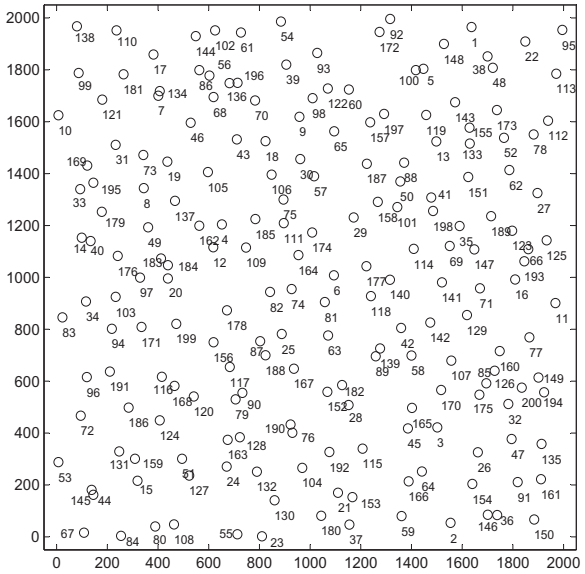

Fig. 7. The topology for a 200-node network.

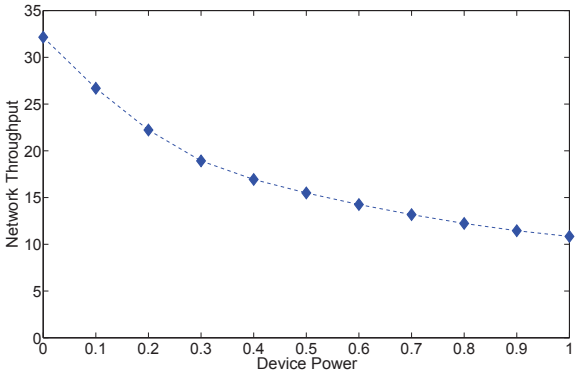

Fig. 8. Network throughput as a function of the device power P_d for the 50-node network.

TABLE II
EACH SESSION'S SOURCE NODE, DESTINATION NODE, AND WEIGHT FOR THE 50-NODE NETWORK.

Session f	Source node $s(f)$	Dest. node $d(f)$	Weight $w(f)$
1	10	35	0.5
2	35	21	0.9
3	5	23	0.7
4	43	14	0.6
5	29	7	0.8

We now vary P_d from 0 to 1 and study how the network throughput changes. The resulting curve is shown in Fig. 8. We can see that the device power has a significant impact on network throughput. Even when P_d changes from 0 to 0.1, the network throughput decreases from 32.18 to 26.30. This confirms our hypothesis that the device power cannot be neglected in the problem formulation.

2) Optimal Throughput-Energy Curve: For the same 50-node network instance, we characterize its optimal throughput-energy curve based on our approach in Section IV. The optimal throughput-energy curve is depicted in Fig. 9, which verifies all three properties as stated in Property 1. As shown in the figure, the curve is nondecreasing. The network throughput

TABLE III
POWER ASSIGNMENT FOR EACH ACTIVE LINK IN THE FINAL SOLUTION FOR THE 50-NODE NETWORK.

Link	Power	Link	Power	Link	Power
$1 \to 27$	0.1832	$1 \to 23$	0.5066	$1 \to 17$	0.4910
$2 \to 45$	0.2003	$2 \to 24$	0.0414	$3 \to 44$	0.2012
$3 \to 13$	0.1750	$3 \to 6$	0.0305	$4 \to 45$	0.1987
$4 \to 22$	0.1493	$4 \to 13$	0.2396	$5 \to 44$	0.2120
$5 \to 8$	0.1835	$5 \to 7$	0.0283	$6 \to 4$	0.5651
$7 \to 15$	0.4338	$7 \to 8$	0.1368	$8 \to 44$	0.0740
$8 \to 15$	0.2590	$8 \to 7$	0.1275	$8 \to 3$	0.5422
$9 \to 43$	0.1589	$9 \to 10$	0.2867	$10 \to 47$	0.2002
$10 \to 42$	0.2853	$10 \to 27$	0.3039	$10 \to 26$	0.0103
$10 \to 9$	0.1919	$10 \to 1$	0.3047	$11 \to 34$	0.2576
$11 \to 32$	0.1568	$13 \to 4$	0.4706	$13 \to 3$	0.0891
$14 \to 22$	0.2455	$15 \to 47$	0.2349	$15 \to 8$	0.5184
$15 \to 7$	0.6236	$17 \to 45$	0.1398	$17 \to 23$	0.0303
$17 \to 14$	0.1447	$22 \to 45$	0.0477	$22 \to 17$	0.3894
$22 \to 14$	0.2639	$24 \to 47$	0.4010	$24 \to 2$	0.0588
$25 \to 37$	0.1337	$26 \to 32$	0.3546	$27 \to 39$	0.4766
$27 \to 10$	0.3217	$27 \to 1$	0.1171	$29 \to 39$	0.5384
$29 \to 34$	0.2134	$29 \to 32$	0.0846	$29 \to 1$	0.6409
$30 \to 25$	0.0824	$32 \to 36$	0.0807	$32 \to 11$	0.2872
$33 \to 43$	0.5296	$34 \to 35$	0.4374	$34 \to 29$	0.2962
$34 \to 11$	0.1407	$35 \to 41$	0.3464	$35 \to 34$	0.3822
$36 \to 30$	0.4168	$37 \to 33$	0.1863	$39 \to 29$	0.0862
$39 \to 27$	0.3252	$39 \to 23$	0.0894	$39 \to 17$	0.5201
$41 \to 14$	0.2582	$42 \to 47$	0.0167	$42 \to 15$	0.1460
$42 \to 10$	0.2679	$43 \to 47$	0.4785	$43 \to 21$	0.4445
$43 \to 9$	0.2374	$44 \to 5$	0.3346	$44 \to 3$	0.5413
$45 \to 22$	0.0387	$45 \to 17$	0.3761	$45 \to 4$	0.1229
$45 \to 2$	0.1409	$47 \to 43$	0.4451	$47 \to 42$	0.0347
$47 \to 24$	0.5701	$47 \to 15$	0.2655		

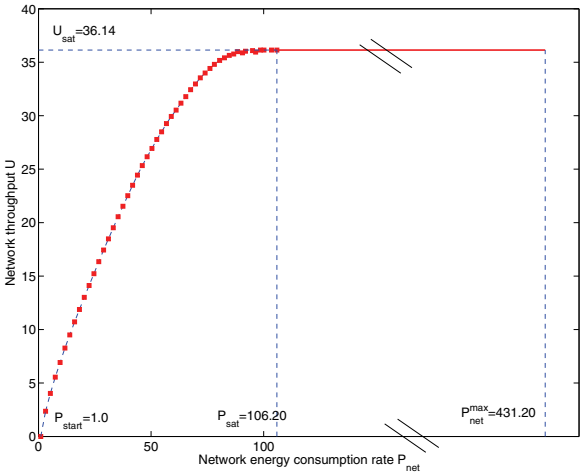

Fig. 9. The optimal throughput-energy curve for the 50-node network, where the "\\" sign in the figure indicates nonlinear scale for $P_{\text{net}} \in [106.20, 431.20]$.

remains at zero when the network energy consumption rate is no greater than P_{start}. For the starting point $(P_{\text{start}}, 0)$, since Session 1 needs at least 5 hops , we have $P_{\text{start}} = 5 \cdot P_d = 1$. For the saturation point $(P_{\text{sat}}, U_{\text{sat}})$, we get $(P_{\text{sat}}, U_{\text{sat}}) = (106.20, 36.14)$. The network throughput ceases to increase and remains at 36.14 when the network energy consumption rate exceeds $P_{\text{sat}} = 106.20$.

C. Results for the 100-node Network

For the 100-node network, we assume that there are $|\mathcal{F}| = 10$ active sessions in the network, with each session's source node, destination node, and weight given in Table V.

TABLE IV
FLOW ROUTING RESULTS FOR THE 50-NODE NETWORK.

Session f	Flow rate on each link attributed to session f
1	$r_{10\to27}(1) = 2.59$, $r_{10\to26}(1) = 1.94$, $r_{11\to34}(1) = 1.94$ $r_{26\to32}(1) = 1.94$, $r_{27\to39}(1) = 2.59$, $r_{29\to34}(1) = 2.59$ $r_{32\to11}(1) = 1.94$, $r_{34\to35}(1) = 4.53$, $r_{39\to29}(1) = 2.59$
2	$r_{1\to27}(2) = 1.54$, $r_{2\to24}(2) = 2.10$, $r_{9\to43}(2) = 1.54$ $r_{10\to9}(2) = 1.54$, $r_{11\to32}(2) = 1.35$, $r_{14\to22}(2) = 2.10$ $r_{22\to45}(2) = 2.10$, $r_{24\to47}(2) = 2.10$, $r_{25\to37}(2) = 2.81$ $r_{27\to10}(1) = 1.54$, $r_{29\to32}(2) = 1.46$, $r_{29\to1}(1) = 1.54$ $r_{30\to25}(2) = 2.81$, $r_{32\to36}(2) = 2.81$, $r_{33\to43}(2) = 2.81$ $r_{34\to29}(1) = 2.99$, $r_{34\to11}(2) = 1.35$, $r_{35\to41}(1) = 2.10$ $r_{35\to34}(2) = 4.34$, $r_{36\to30}(1) = 2.81$, $r_{37\to33}(1) = 2.81$ $r_{41\to14}(1) = 2.10$, $r_{43\to21}(1) = 6.45$, $r_{45\to2}(1) = 2.10$ $r_{47\to43}(1) = 2.10$
3	$r_{1\to23}(3) = 2.10$, $r_{1\to17}(3) = 0.32$, $r_{2\to45}(3) = 0.32$ $r_{3\to13}(3) = 2.99$, $r_{3\to6}(3) = 2.59$, $r_{4\to45}(3) = 2.75$ $r_{4\to22}(3) = 2.83$, $r_{5\to44}(3) = 1.70$, $r_{5\to8}(3) = 3.07$ $r_{5\to7}(3) = 4.29$, $r_{6\to4}(3) = 2.59$, $r_{7\to15}(3) = 1.94$ $r_{7\to8}(3) = 2.35$, $r_{8\to44}(3) = 1.70$, $r_{8\to15}(3) = 1.54$ $r_{8\to3}(3) = 2.18$, $r_{10\to27}(3) = 1.54$, $r_{10\to1}(3) = 1.62$ $r_{13\to4}(3) = 2.99$, $r_{15\to47}(3) = 3.48$, $r_{17\to23}(3) = 6.23$ $r_{22\to45}(3) = 0.32$, $r_{22\to17}(3) = 2.51$, $r_{24\to2}(3) = 0.32$ $r_{27\to39}(3) = 0.73$, $r_{27\to1}(3) = 0.81$, $r_{39\to23}(3) = 0.73$ $r_{42\to10}(3) = 3.15$, $r_{44\to3}(3) = 3.40$, $r_{45\to17}(3) = 3.40$ $r_{47\to42}(3) = 3.15$, $r_{47\to24}(3) = 0.32$
4	$r_{1\to17}(4) = 1.94$, $r_{2\to45}(4) = 2.18$, $r_{9\to10}(4) = 1.94$ $r_{10\to27}(4) = 1.94$, $r_{17\to14}(4) = 1.94$, $r_{22\to14}(4) = 2.18$ $r_{24\to2}(4) = 2.18$, $r_{27\to1}(4) = 1.94$, $r_{43\to47}(4) = 2.18$ $r_{43\to9}(4) = 1.94$, $r_{45\to22}(4) = 2.18$, $r_{47\to24}(4) = 2.18$
5	$r_{1\to27}(5) = 1.78$, $r_{3\to44}(5) = 2.18$, $r_{4\to13}(5) = 2.18$ $r_{5\to7}(5) = 2.18$, $r_{8\to7}(5) = 2.26$, $r_{10\to47}(5) = 1.38$ $r_{10\to42}(5) = 3.24$, $r_{13\to3}(5) = 2.18$, $r_{15\to8}(5) = 2.26$ $r_{15\to7}(5) = 2.35$, $r_{17\to45}(5) = 2.18$, $r_{27\to10}(5) = 4.61$ $r_{29\to39}(5) = 5.02$, $r_{29\to1}(5) = 1.78$, $r_{39\to27}(5) = 2.83$ $r_{39\to17}(5) = 2.18$, $r_{42\to47}(5) = 2.26$, $r_{42\to15}(5) = 0.97$ $r_{44\to5}(5) = 2.18$, $r_{45\to4}(5) = 2.18$, $r_{47\to15}(5) = 3.64$

We assume that the maximum network-wide energy consumption rate is given by $P_{\text{net}} = 60$. By employing our method, we obtain that the maximum network throughput is $U = 34.49$. The achieved session data rates are $r_1 = 9.68$, $r_2 = 2.76$, $r_3 = 7.07$, $r_4 = 2.52$, $r_5 = 9.40$, $r_6 = 4.00$, $r_7 = 2.30$, $r_8 = 2.57$, $r_9 = 7.82$, and $r_{10} = 3.39$. The detailed results for power assignment and flow routing are given in Tables VI and VII, respectively. The above numerical results were obtained when $P_d = 0.2$. We also show in Fig. 11 how the throughput changes for the 100-node network with $P_d = 0.2$ as the device power varies.

D. Results for the 200-node Network

For the 200-node network, we assume that there are $|\mathcal{F}| = 12$ active sessions in the network, with each session's source node, destination node, and weight given in Table VIII.

We assume that the maximum network-wide energy consumption rate is given by $P_{\text{net}} = 160$. By employing our method, we obtain that the maximum network throughput is $U = 78.84$. The achieved session data rates are $r_1 = 15.23$, $r_2 = 10.27$, $r_3 = 9.70$, $r_4 = 11.84$, $r_5 = 13.07$, $r_6 = 1.86$, $r_7 = 10.14$, $r_8 = 2.67$, $r_9 = 7.09$, $r_{10} = 1.04$, $r_{11} = 27.67$, and $r_{12} = 6.06$. The detailed results for power assignment and flow routing are omitted to conserve space. The device power and throughput curve and the optimal throughput-energy curve follow a similar pattern as for the 50- and 100-node network, which are also omitted here for the sake of brevity.

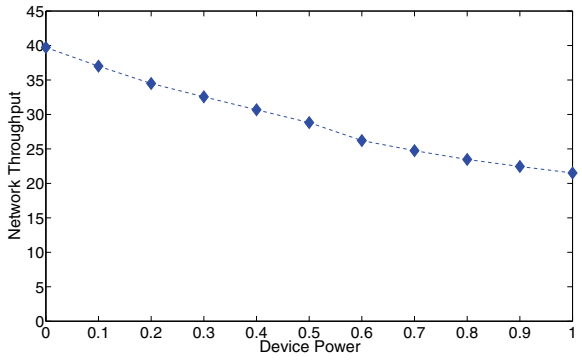

Fig. 10. Network throughput as a function of the device power for the 100-node network.

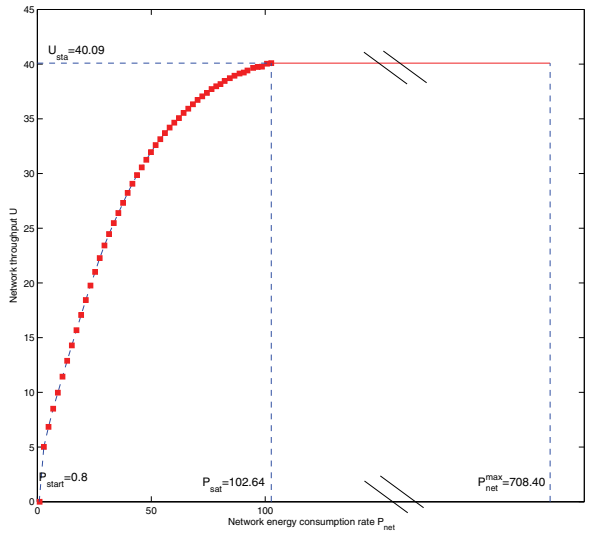

Fig. 11. The optimal throughput-energy curve for the 100-node network, where the "\\" sign in the figure indicates nonlinear scale for $P_{\text{net}} \in [102.64, 708.40]$.

VI. Conclusions

This paper has explored problems associated with total network energy, an area that is of great significance to network operators but has not been well studied by the research community. Specifically, we examined the following two problems. In the first problem, we studied how to maximize network throughput under a network-wide energy constraint. We formulated this problem as a mixed-integer nonlinear program (MINLP) and proposed a near-optimal solution procedure with a guaranteed performance bound that is asymptotically optimal. In the second problem, we explored the joint optimization of both network throughput and energy consumption via a multicriteria optimization framework. We showed how to generate weakly Pareto-optimal solutions in order to characterize an optimal throughput-energy curve. In our study, we have considered the device power associated with an active link, which turns out to be a significant factor that affects throughput performance but has been overlooked in prior efforts. The results in this paper offer both theoretical solutions and practical insights to network operators when total energy consumption is of interest while maximizing network throughput.

TABLE V
EACH SESSION'S SOURCE NODE, DESTINATION NODE, AND WEIGHT FOR THE 100-NODE NETWORK.

Session f	Source node $s(f)$	Dest. node $d(f)$	Weight $w(f)$
1	40	26	0.9
2	27	17	0.8
3	4	55	0.7
4	31	41	0.2
5	78	100	0.8
6	7	83	0.6
7	73	91	0.3
8	12	10	0.4
9	64	38	0.6
10	51	56	0.5

TABLE VI
POWER ASSIGNMENT FOR EACH ACTIVE LINK IN THE FINAL SOLUTION FOR THE 100-NODE NETWORK.

Link	Power	Link	Power	Link	Power
$1 \to 42$	0.2149	$2 \to 7$	0.2222	$3 \to 91$	0.5415
$4 \to 83$	1.0234	$4 \to 8$	0.9766	$6 \to 99$	0.0232
$6 \to 34$	0.2688	$7 \to 74$	1.4991	$7 \to 42$	0.3606
$8 \to 83$	0.1404	$8 \to 11$	0.2158	$11 \to 52$	0.1615
$11 \to 23$	0.3240	$12 \to 71$	0.3392	$13 \to 56$	1.6038
$14 \to 55$	0.0315	$14 \to 3$	0.5382	$15 \to 90$	0.9677
$15 \to 1$	1.0323	$18 \to 89$	0.2942	$20 \to 38$	2.0000
$23 \to 65$	0.1818	$23 \to 41$	0.2434	$27 \to 18$	0.1185
$28 \to 52$	0.0176	$28 \to 39$	0.3859	$29 \to 38$	1.5862
$30 \to 85$	0.5012	$30 \to 43$	0.2242	$31 \to 60$	0.1188
$34 \to 99$	0.1345	$34 \to 67$	0.3060	$34 \to 6$	0.1601
$36 \to 100$	0.3526	$39 \to 68$	0.3097	$40 \to 47$	1.1874
$40 \to 30$	0.8126	$41 \to 26$	0.5198	$42 \to 74$	0.9261
$42 \to 46$	0.1153	$42 \to 36$	0.9586	$43 \to 85$	0.3057
$45 \to 72$	1.5655	$46 \to 94$	0.3396	$46 \to 42$	0.0473
$47 \to 86$	0.6319	$47 \to 17$	0.4046	$48 \to 13$	0.1070
$51 \to 99$	0.8480	$52 \to 65$	0.2639	$52 \to 28$	0.0243
$52 \to 23$	0.2692	$54 \to 10$	0.7201	$55 \to 68$	0.2972
$56 \to 76$	0.0261	$60 \to 28$	0.4521	$64 \to 67$	0.3104
$64 \to 48$	0.0627	$65 \to 77$	0.4445	$66 \to 73$	0.6573
$67 \to 76$	1.4814	$67 \to 34$	0.5186	$68 \to 55$	0.3907
$68 \to 54$	0.7710	$71 \to 14$	0.0362	$72 \to 2$	0.2333
$73 \to 41$	0.3026	$73 \to 14$	0.5069	$74 \to 100$	0.3338
$74 \to 36$	0.0155	$76 \to 56$	0.0236	$76 \to 29$	0.2422
$77 \to 55$	0.3670	$78 \to 45$	0.9702	$78 \to 15$	0.1884
$79 \to 40$	0.7875	$83 \to 11$	0.0566	$85 \to 26$	2.0000
$86 \to 95$	0.0144	$89 \to 79$	0.2912	$90 \to 94$	0.1828
$94 \to 83$	1.8608	$94 \to 46$	0.1392	$95 \to 66$	0.4048
$99 \to 20$	0.3262	$99 \to 6$	0.0390		

In this study, we have employed orthogonal channels to simplify scheduling at the link layer. However, our proposed solution may also be extended to solve problems under more complex interference situations. For example, we could extend our approach to the interference models proposed in [15], [18]. In these models, the network was represented as a directed graph, where the vertices represent the nodes and the links represent the communication links. A node can only receive from or transmit to at most one node in any time-slot. Under such an interference model, we can introduce suitable binary variables and use linear constraints to characterize the node-exclusive interference relationship in the network. In this case, the problem formulation will still be an MINLP. It will have more linear constraints, but the same set of nonlinear constraints as those in the present paper (i.e., based on logarithmic functions for computing the link capacities). Therefore, we can likewise apply the linear approximation technique proposed herein to transform such an MINLP into an MILP and solve it thereby to derive a near-optimal solution.

TABLE VII
FLOW ROUTING RESULTS FOR THE 100-NODE NETWORK.

Session f	Flow rate on each link attributed to session f
1	$r_{30\to85}(1)=3.00$, $r_{30\to43}(1)=3.78$, $r_{40\to47}(1)=2.90$ $r_{40\to30}(1)=6.77$, $r_{41\to26}(1)=2.90$, $r_{43\to85}(1)=3.78$ $r_{47\to86}(1)=2.90$, $r_{66\to73}(1)=2.90$, $r_{73\to41}(1)=2.90$ $r_{85\to26}(1)=6.77$, $r_{86\to95}(1)=2.90$, $r_{95\to66}(1)=2.90$
2	$r_{18\to89}(2)=2.76$, $r_{27\to18}(2)=2.76$, $r_{40\to47}(2)=2.76$ $r_{47\to17}(2)=2.76$, $r_{79\to40}(2)=2.76$, $r_{89\to79}(2)=2.76$
3	$r_{4\to83}(3)=3.23$, $r_{4\to8}(3)=3.84$, $r_{8\to83}(3)=1.59$ $r_{8\to11}(3)=2.24$, $r_{11\to52}(3)=4.33$, $r_{11\to23}(3)=2.74$ $r_{23\to65}(3)=2.74$, $r_{28\to39}(3)=2.91$, $r_{39\to68}(3)=2.91$ $r_{52\to65}(3)=1.42$, $r_{52\to28}(3)=2.91$, $r_{65\to77}(3)=4.16$ $r_{68\to55}(3)=2.91$, $r_{77\to55}(3)=4.16$, $r_{83\to11}(3)=4.82$
4	$r_{23\to41}(4)=2.52$, $r_{28\to52}(4)=2.52$, $r_{31\to60}(4)=2.52$ $r_{52\to23}(4)=2.52$, $r_{60\to28}(4)=2.52$
5	$r_{1\to42}(5)=2.96$, $r_{2\to7}(5)=3.60$, $r_{7\to74}(5)=3.38$ $r_{7\to42}(5)=0.22$ $r_{15\to90}(5)=2.84$, $r_{15\to1}(5)=2.96$ $r_{36\to100}(5)=6.13$, $r_{42\to74}(5)=3.01$, $r_{42\to36}(5)=3.00$ $r_{45\to72}(5)=3.60$, $r_{46\to42}(5)=2.84$, $r_{72\to2}(5)=3.60$ $r_{74\to100}(5)=3.27$, $r_{74\to36}(5)=3.13$, $r_{78\to45}(5)=3.60$ $r_{78\to15}(5)=5.80$, $r_{90\to94}(5)=2.84$, $r_{94\to46}(5)=2.84$
6	$r_{7\to42}(6)=4.00$, $r_{42\to46}(6)=4.00$, $r_{46\to94}(6)=4.00$ $r_{94\to83}(6)=4.00$
7	$r_{3\to91}(7)=2.30$, $r_{14\to3}(7)=2.30$, $r_{73\to14}(7)=2.30$
8	$r_{12\to71}(8)=2.57$, $r_{14\to55}(8)=2.57$, $r_{54\to10}(8)=2.57$ $r_{55\to68}(8)=2.57$, $r_{68\to54}(8)=2.57$, $r_{71\to14}(8)=2.57$
9	$r_{6\to99}(9)=2.74$, $r_{13\to56}(9)=3.53$, $r_{20\to38}(9)=4.10$ $r_{29\to38}(9)=3.72$, $r_{34\to99}(9)=1.36$, $r_{34\to6}(9)=2.74$ $r_{48\to13}(9)=3.53$, $r_{56\to76}(9)=3.53$, $r_{64\to67}(9)=4.29$ $r_{64\to48}(9)=3.53$, $r_{67\to76}(9)=0.20$, $r_{67\to34}(9)=4.10$ $r_{76\to29}(9)=3.72$, $r_{99\to20}(9)=4.10$
10	$r_{6\to34}(10)=3.39$, $r_{34\to67}(10)=3.39$, $r_{51\to99}(10)=3.39$ $r_{67\to76}(10)=3.39$, $r_{76\to56}(10)=3.39$, $r_{99\to6}(10)=3.39$

TABLE VIII
EACH SESSION'S SOURCE NODE, DESTINATION NODE, AND WEIGHT FOR THE 200-NODE NETWORK.

Session f	Source node $s(f)$	Dest. node $d(f)$	Weight $w(f)$
1	35	21	0.9
2	115	23	0.7
3	43	114	0.6
4	29	7	0.8
5	58	25	0.5
6	147	99	0.9
7	3	62	0.7
8	137	17	0.4
9	78	65	0.5
10	147	99	0.9
11	183	162	0.5
12	137	17	0.9

ACKNOWLEDGMENTS

The work of Y.T. Hou and H.D. Sherali was supported in part by NSF grants 0925719 and 1064953. The work of W. Lou was supported in part by NSF grants 1156311 and 1156318.

APPENDIX

Proof of Lemma 2 Our proof is based on contradiction. Assume that the number of linear segments that Algorithm 1 generates is K_l, and $s_l^{(k)}, k=0,\ldots,K_l$, are the corresponding s_l-axis end-point values. Suppose that there is another piecewise linear approximation that needs $K_l' < K_l$ linear segments with $t_l^{(k)}(\ k=0,\ldots,K_l'$, $t_l^{(0)}=0$ and $t_l^{(K_l')}=s_l^{\max})$ being the corresponding s_l-axis values at the end-points.

Since $s_l^{(1)}$ is the largest possible s_l-axis value of the second end-point given the ϵ-tolerance, we have that $t_l^{(1)} \le s_l^{(1)}$. By induction, we can show that $t_l^{(k)} \le s_l^{(k)}, k=1,\ldots,K_l'$. For $k=K_l'$, we have $t_l^{(K_l')} \le s_l^{(K_l')}$. Furthermore, since $K_l' < K_l$, we also have $s_l^{(K_l')} < s_l^{\max}$. Therefore, we conclude that $t_l^{(K_l')} \le s_l^{(K_l')} < s_l^{\max}$, which is a contradiction to $t_l^{(K_l')} = s_l^{\max}$. This completes the proof. □

Proof of Lemma 3 Note that the only difference between OPT and OPT-R is with respect to the link capacity constraints. Each link capacity constraint for link l in OPT is replaced by a set of linear constraints in OPT-R. Since these linear constraints are generated by the piece-wise linear segments lying beneath the log curve, the feasible region of OPT-R is contained within the feasible region of OPT. Thus, a feasible solution to OPT-R is also a feasible solution to OPT. □

REFERENCES

[1] M. Andrews and M. Dinitz, "Maximizing capacity in arbitrary wireless networks in the SINR model: complexity and game theory," in *Proc. 2009 IEEE INFOCOM,* pp. 1332–1340.

[2] M. S. Bazaraa, J. J. Jarvis, and H. D. Sherali, *Linear Programming and Network Flows*, 4th edition. John Wiley & Sons Inc., 2010.

[3] L. Chen, S. H. Low, M. Chiang, and J. C. Doyle, "Cross-layer congestion control, routing and scheduling design in ad hoc wireless networks," in *Proc. 2006 IEEE INFOCOM*.

[4] IBM ILOG CPLEX Optimizer, http://www-01.ibm.com/software/integration/optimization/cplex-optimizer/.

[5] S. Cui, A. J. Goldsmith, and A. Bahai, "Energy-constrained modulation optimization," *IEEE Trans. Wireless Commun.*, vol. 4, no. 5, pp. 2349–2360, Sep. 2005.

[6] M. Ehrgott, *Multicriteria Optimization*, 2nd edition. Springer-Verlag, 2010.

[7] R. Fletcher and S. Leyffer, "Solving mixed integer programs by outer approximation," *Mathematical Programming,* vol. 66, no. 1–3, pp. 327–349, 1994.

[8] O. K. Gupta and A. Ravindran, "Branch and bound experiments in convex nonlinear integer programming," *Management Science,* vol. 31, no. 12, pp. 1533–1546, 1985.

[9] S. Huang, X. Liu, and Z. Ding, "Distributed power control for cognitive user access based on primary link control feedback," in *Proc. 2010 IEEE INFOCOM,* pp. 1280–1288.

[10] M. R. Garey and D. S. Johnson, *Computers and Intractability: A Guide to the Theory of NP-completeness.* W. H. Freeman and Company, pp. 245–248, 1979.

[11] A. M. Geoffrion, "A generalized Benders' decomposition," *J. Optimization Theory and Applications,* vol. 10, no. 4, pp. 237–260, 1972.

[12] C. Jiang, Y. Shi, Y. T. Hou, and W. Lou, "Cherish every Joule: maximizing throughput with an eye on network-wide energy consumption," in *Proc. 2012 IEEE INFOCOM,* pp. 1934–1941.

[13] M. Kodialam and T. Nandagopal, "Characterizing achievable rates in multi-hop wireless mesh networks with orthogonal channels," *IEEE/ACM Trans. Networking,* vol. 13, no. 4, pp. 868–880, Aug. 2005.

[14] B. Li, Y. T. Hou, J. Liu, G. D. Nguyen, and T. F. Znati (Guest Editors), *ACM/Kluwer Mobile Networks and Applications,* vol. 10, no. 6, Dec. 2005.

[15] L. Lin, X. Lin, and N. B. Shroff, "Low-complexity and distributed energy minimization in multihop wireless networks," *IEEE/ACM Trans. Networking,* vol. 18, no. 2, pp. 501–514, Apr. 2010.

[16] I. Maric and R. D. Yates, "Cooperative multihop broadcast for wireless networks," *IEEE J. Sel. Areas Commun.*, vol. 22, no. 6, pp. 1080–1088, Aug. 2004.

[17] G. W. Miao, N. Himayat, and G. Y. Li, "Energy-efficient link adaptation in frequency-selective channels," *IEEE Trans. Commun.*, vol. 58, no. 2, pp. 545–554, Feb. 2010.

[18] M. J. Neely, "Energy optimal control for time varying wireless networks," *IEEE Trans. Inf. Theory,* vol. 52, no. 7, pp. 2915–2934, July 2006.

[19] S. Rosloniec, *Fundamental Numerical Methods for Electrical Engineering.* Springer, 2008.

[20] Y. Shi, Y. T. Hou, S. Kompella, and H. D. Sherali, "Maximizing capacity in multi-hop cognitive radio networks under the SINR model," *IEEE Trans. Mobile Computing,* vol. 10, no. 7, pp. 954–967, July 2011.

[21] J. Tang, G. Xue, C. Chandler, and W. Zhang, "Link scheduling with power control for throughput enhancement in multihop wireless networks," *IEEE Trans. Veh. Technol.*, vol. 55, no. 3, pp. 733–742, May 2006.

[22] T. Westerlund and F. Pettersson, "An extended cutting plane method for solving convex MINLP problems," *Computers Chem. Eng.,* vol. 19, supplement 1, pp. 131–136, 1995.

[23] J. E. Wieselthier, G. D. Nguyen, and A. Ephremides, "Energy-aware wireless networking with directional antennas: the case of session-based broadcasting and multicasting," *IEEE Trans. Mobile Computing,* vol. 1, no. 3, pp. 176–192, July–Sept. 2002.

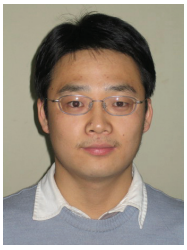

Canming Jiang (S'08) received the B.E. degree in Electrical Engineering and Information Science from the University of Science and Technology of China, Hefei, China, in 2004, the M.S. degree in Computer Science from the Graduate School, Chinese Academy of Sciences, Beijing, China, in 2007, and the Ph.D. degree in Computer Engineering from Virginia Tech, Blacksburg, VA, in 2012. His research interests are to explore new fundamental understandings of emerging wireless networks, such as cognitive radio networks and MIMO wireless networks.

Yi Shi (S'02–M'08) received his Ph.D. degree in Computer Engineering from Virginia Tech, Blacksburg, VA in 2007. He is currently an Adjunct Assistant Professor in the Bradley Department of Electrical and Computer Engineering at Virginia Tech.

Dr. Shi's research focuses on algorithms and optimization for cognitive radio networks, MIMO and cooperative communication networks, sensor networks, and ad hoc networks. He was a recipient of IEEE INFOCOM 2008 Best Paper Award, the only IEEE INFOCOM 2011 Best Paper Award Runner-up, and Chinese Government Award for Outstanding Ph.D. Students Abroad (2006). He serve on technical program committee on some major international conferences (including ACM MobiHoc and IEEE INFOCOM).

Y. Thomas Hou (S'91–M'98–SM'04) received his Ph.D. degree in Electrical Engineering from Polytechnic Institute of New York University in 1998. From 1997 to 2002, Dr. Hou was a Researcher at Fujitsu Laboratories of America, Sunnyvale, CA. Since 2002, he has been with Virginia Polytechnic Institute and State University ("Virginia Tech"), the Bradley Department of Electrical and Computer Engineering, Blacksburg, VA, where he is now a Professor.

Prof. Hou's research interests are cross-layer optimization for wireless networks. Specifically, he is most interested in how to make significant improvement for network layer performance by exploiting new advances at the physical layer. He has published extensively in leading IEEE journals and top-tier IEEE/ACM conferences and received five best paper awards from IEEE (including IEEE INFOCOM 2008 Best Paper Award and IEEE ICNP 2002 Best Paper Award). Prof. Hou is currently serving as an Area Editor of IEEE TRANSACTIONS ON WIRELESS COMMUNICATIONS, and Editor for IEEE TRANSACTIONS ON MOBILE COMPUTING and *IEEE Wireless Communications.* He was Technical Program Co-Chair of IEEE INFOCOM 2009. Prof. Hou co-edited a textbook titled *Cognitive Radio Communications and Networks: Principles and Practices,* which was published by Academic Press/Elsevier, 2010.

Wenjing Lou (S'01–M'03–SM'08) is an associate professor at Virginia Polytechnic Institute and State University. Prior to joining Virginia Tech in 2011, she was on the faculty of Worcester Polytechnic Institute from 2003 to 2011. She received her Ph.D. in Electrical and Computer Engineering at the University of Florida in 2003. Her current research interests are in cyber security, with emphases on wireless network security and data security and privacy in cloud computing. She was a recipient of the U.S. National Science Foundation CAREER award in 2008.

Hanif D. Sherali is a University Distinguished Professor and the W. Thomas Rice Chaired Professor of Engineering in the Industrial and Systems Engineering Department at Virginia Polytechnic Institute and State University. His areas of research interest are in analyzing problems and designing algorithms for specially structured linear, nonlinear, and integer programs arising in various applications, global optimization methods for non-convex programming problems, location and transportation theory and applications, economic and energy mathematical modeling and analysis. He has published over two hundred refereed articles in various Operations Research journals, has (co-) authored six books in this area, and serves on the editorial board of eight journals. He is an elected member of the U.S National Academy of Engineering.